Carbohydrate Polymers 101 (2014) 812–818

Contents lists available at ScienceDirect

Carbohydrate Polymers

journal homepage: www.elsevier.com/locate/carbpol

The green adsorption of chitosan tripolyphosphate nanoparticles on cotton fiber surfaces

Mingxi Wang[a], Yuanbin She[a,b,*], Zuobing Xiao[c], Jing Hu[c], Rujun Zhou[c], Jia Zhang[c]

[a] Institute of Green Chemistry and Fine Chemicals, Beijing University of Technology, Beijing 100124, PR China
[b] Key Laboratory of Catalysis and Materials Science of the State Ethnic Affairs Commission & Ministry of Education, South-Central University for Nationalities, Wuhan 430074, PR China
[c] School of Perfume and Aroma Technology, Shanghai Institute of Technology, Shanghai 201418, PR China

ARTICLE INFO

Article history:
Received 18 June 2013
Received in revised form 6 October 2013
Accepted 7 October 2013
Available online 15 October 2013

Keywords:
Chitosan nanoparticle
Cotton fiber
Interaction
Hydrogen bond
Adsorption without cross-linking agents

ABSTRACT

Chitosan nanoparticles (chitosan NP) were effectively incorporated onto cotton fiber surfaces during a green adsorption without any cross-linking agents in this work. The interactions between cotton fibers and chitosan NP during the green adsorption were investigated by Fourier transform infrared spectroscopy (FTIR), X-ray photoelectron spectroscopy (XPS), X-ray diffraction (XRD), thermogravimetric-derivative thermogravimetry (TG-DTG) and scanning electron microscopy (SEM) in detail. The results indicated that the intermolecular hydrogen bond interactions exited between the hydroxyl groups of cotton fibers and the amino groups of chitosan NP, and progressively enhanced with the increase in chitosan NP mass concentrations. After chitosan NP adsorption, the acidity of fibers augmented and the crystallinity index of fibers declined owing to the increasing interactions. In addition, the hydrophobic interactions occurred between chitosan NP and crystalline cotton fibers, thereby resulting in the preferential adsorption onto the hydrophobic (2 0 0) crystallographic plane.

1. Introduction

Chitosan is the linear and typically 20% acetylated (1-4)-2-amino-2-deoxy-β-D-glucan, and it is obtained from chitin (Muzzarelli, 2012; Muzzarelli et al., 2012). Recently, chitosan has been reported to be an excellent biopolymer for preparing nanoparticles due to its superior biodegradability, biocompatibility and mucoadhesive property (Hejazi & Amiji, 2003; Lehr, Bouwstra, Schacht, & Junginger, 1992; Vila, Sánchez, Tobío, Calvo, & Alonso, 2002). Chitosan nanoparticles (chitosan NP) have been extensively investigated as sustained-release carriers in gene and drug-delivery systems (Gan, Wang, Cochrane, & McCarron, 2005; Katas & Alpar, 2006; Papadimitriou, Bikiaris, Avgoustakis, Karavas, & Georgarakis, 2008; Saboktakin, Tabatabaee, Maharramov, & Ramazanov, 2010; Zhang, Oh, Allen, & Kumacheva, 2004) and utilized in the fabrication of functional cotton fabrics (Bashar & Khan, 2013). Owing to the large surface area to volume ratio and high surface energy (Rajendran, Radhai, Kotresh, & Csiszar, 2013), the nanoparticles had a good affinity for cotton fabrics and could be finished on the fiber surface without any chemical cross-linking agents which generally contained certain harmful and hazardous compounds. After chitosan NP treatment, the cotton fabric exhibited an excellent antibacterial (Rajendran et al., 2013; Ye, Xin, Li, Lee, & Kwong, 2006) or superhydrophobic property (Ivanova & Philipchenko, 2012). Meanwhile, an aromatic cotton fabric with good laundering durability and sustained fragrance release was prepared via the green adsorption of fragrance-loaded chitosan NP (Hu et al., 2012).

However, most of the previous studies focused on the performance and application of modified cotton fabrics via chitosan NP treatment. The mechanism of the green adsorption process without cross-linking agents has not been clear. The several studies on the preparation and characterization of chitosan–cellulose films or nanocomposites (Da Róz et al., 2010; Mesquita, Donnici, & Pereira, 2010; Li, Zhou, & Zhang, 2009; Phisalaphong & Jatupaiboon, 2008; Rosca, Popa, Lisa, & Chitanu, 2005; Ul-Islam, Shah, Ha, & Park, 2011; Wu et al., 2004) have been reported. The results from these studies demonstrated that intermolecular hydrogen bonding (De Mesquita et al., 2010; Phisalaphong & Jatupaiboon, 2008; Ul-Islam et al., 2011; Wu et al., 2004) and electrostatic interactions (Da Róz et al., 2010; De Mesquita et al., 2010; Li et al., 2009; Rosca et al., 2005) occurred between chitosan and cellulose, consequently leading to the good miscibility between the two components. On the basis of these reports, a probable adsorption mechanism between cotton fabrics and chitosan NP was assumed in our previous study (Hu et al., 2012). It showed that the nanoparticles could penetrate into the 50–200 nm holes (Rous, Ingolic, & Schuster, 2006) on fiber

* Corresponding author at: Institute of Green Chemistry and Fine Chemicals, Beijing University of Technology, Beijing 100124, PR China. Tel.: +86 10 67392695; fax: +86 10 67392695.
E-mail addresses: sheyb@bjut.edu.cn, frankybshe@163.com (Y. She).

0144-8617/$ – see front matter © 2013 Elsevier Ltd. All rights reserved.
http://dx.doi.org/10.1016/j.carbpol.2013.10.023

surfaces depending on osmotic pressures and the hydrogen bonds potentially developed between the hydroxyl groups of chitosan NP and cellulose. Additionally, the study from Ye et al. (2006) inferred that the chitosan NP could adhere firmly onto the cotton fabrics, most probably not only by physical interactions but also by certain chemical bindings. To further comprehend the adsorption mechanism, the current paper is aimed to study the interactions occurring between cotton fibers and chitosan NP during the green adsorption.

2. Experimental

2.1. Materials

Chitosan was purchased from Golden-Shell Biochemical Co. Ltd. (Zhejiang, China) with an average molecular weight of 150 kDa and a deacetylation degree of 90%. Sodium tripolyphosphate was purchased from Sinopharm Chemical Reagent Co. Ltd. (Shanghai, China). The other chemical reagents used in the study were all of analytical reagent grade. Cotton fabric was purchased from Hongdou Group Co. Ltd. (Jiangsu, China) with a specific weight of 120 ± 5 g/m^2 and a thickness of 0.5 mm. Before use, the cotton fabric was cleaned by deionized water at 25 °C for 0.5 h and sodium carbonate solution of 2.0 g/L at 95 °C for 2 h. The rinsed cotton was air-dried at 25 °C for 48 h.

2.2. Formation of chitosan nanoparticles

Chitosan NP were prepared by the ionic gelation process based on the report by Calvo, Remuñán-López, Vila-Jato, and Alonso (1997). The chitosan solutions with different mass concentrations (0.7, 1.4, 2.1, 2.8 g/L) were prepared by dissolving purified chitosan in 1% (w/w) acetic acid solution with sonication at 800 W for 15 min. The pH of chitosan solutions was adjusted to 5.25 with NaOH solution (1 mol/L). The chitosan NP suspension was spontaneously formed by adding dropwise the 45 mL sodium tripolyphosphate solution into the 105 mL chitosan solution under a magnetic stir of 250 rpm at room temperature for 60 min, keeping the weight ratio of chitosan to sodium tripolyphosphate at 5:1.

2.3. Adsorption of chitosan NP on cotton fibers

The neat cotton of 0.5 g was immersed in the 150 mL chitosan NP suspension with a different mass concentration (0.6, 1.2, 1.8, 2.4 g/L). The temperature and pH of the chitosan NP suspension were kept at 25 °C and 6.5, respectively. Without chemical cross-linking agents, the green adsorption was carried out under magnetic stirring at 250 rpm for 60 min to obtain the chitosan NP-adsorbed cotton (chitosan NP-cotton). The treated cotton was air-dried at 25 °C for 48 h before the next characterization.

2.4. Characterization

2.4.1. Fourier transform infrared spectroscopy (FTIR)

Fourier transform infrared spectroscopy (FTIR) spectra of all samples were obtained with a VERTEX70 spectrophotometer (BRUKER, Germany) in the wavenumber range of 4000–600 cm^{-1} to determine the functional groups of chitosan NP-cotton and interactions between chitosan NP and cotton fibers. The dried powders of chitosan NP obtained via freeze drying for 20 h were mixed with potassium bromide to form tablet samples.

2.4.2. X-ray photoelectron spectroscopy (XPS)

In order to reveal the surface chemical changes of chitosan NP-cotton, X-ray photoelectron spectroscopy (XPS) analysis was performed using an AXIS ULTRA^{DLD} photoelectron spectrometer (Kratos, Japan) equipped with monochromatic Al Kα radiation. The spectrometer was operated at 150 W, 15 kV and 15 mA. The photon energy was 1486.6 eV. A pass energy of 80 eV was used in high-resolution scans of C 1s and N 1s region. All calculated binding energy values were relative to the C 1s photoelectron emission signal occurring at 284.8 eV.

2.4.3. X-ray diffraction (XRD)

The crystalline structure of chitosan NP-cotton, as one of the most important parameters for understanding the green adsorption, was characterized by X-ray diffraction (XRD) using an X' Pert PW 3040 diffractometer (PANalytical, Netherlands). The patterns were recorded in the region of 2θ from 10° to 30° with Cu Kα ($\lambda = 0.15406$ nm) radiation at 40 kV and 40 mA. The values of the crystallinity index (*CrI*) of all samples were determined by the surface method (Eq. (1)).

$$CrI \quad (\%) = \frac{S_C}{S_T} \times 100 \tag{1}$$

where S_C is the crystallinity area and S_T is the total area.

2.4.4. Thermogravimetric-derivative thermogravimetry (TG-DTG)

Thermal analyses of all samples were carried out by thermogravimetric-derivative thermogravimetry (TG-DTG) using a Q5000 thermal analyzer (TA Instruments, USA) to determine the interactions between chitosan NP and cotton fibers. The chitosan NP were freeze-dried for 20 h to obtain the powdered samples. Each sample of approximately 4 mg was heated from 30 to 600 °C at a heating rate of 10 °C/min under a constant flow of nitrogen.

2.4.5. Scanning electron microscopy (SEM)

The morphology of the cotton fiber after chitosan NP adsorption was observed by an S-3400N scanning electron microscopy (SEM, HITACHI, Japan) under an accelerating voltage of 15 kV. Each sample was coated with a thin layer of uttered gold particles before observation.

3. Results and discussion

3.1. FTIR analysis

FTIR spectra of chitosan NP, neat cotton and chitosan NP-cotton treated with different chitosan NP mass concentrations were shown in Fig. 1. The overlapped absorption bands in the region of 3200–3520 cm^{-1} were assigned to the O—H and N—H stretching vibrations of cotton fibers and chitosan NP, respectively, as shown in Fig. 1a. After chitosan NP adsorption, the broadband moved slightly and became broader compared to the band of neat cotton. Meanwhile it got increasingly weaker as the content of chitosan NP increased. The results suggested that the intermolecular hydrogen bonds were formed between chitosan NP and cotton fibers (De Mesquita et al., 2010) and gradually enhanced with the increasing chitosan NP mass concentration. The probable mechanism has been proposed that the intermolecular hydrogen bonds of cellulose are broken down to form cellulose–chitosan hydrogen bonds, while the intramolecular and intrastrand hydrogen bonds hold the network flat of cellulose (Wu et al., 2004). Besides, the displacement of bands could also be attributed to the electrostatic interactions between the positively charged amino groups of chitosan and the negatively charged sulfate groups of fiber surface (Li et al., 2009).

In Fig. 1b the FTIR spectra of chitosan NP, neat cotton and chitosan NP-cotton at the wavenumber ranging from 1710 to 1500 cm^{-1} were shown. The absorption in the spectrum of neat cotton was the band at 1640 cm^{-1}, which was attributed to the O—H vibration band of the water present in cellulose (Watanabe et al., 2006). From the spectrum of chitosan NP, the characteristic absorption bands at 1635 cm^{-1} and 1535 cm^{-1} were assigned to

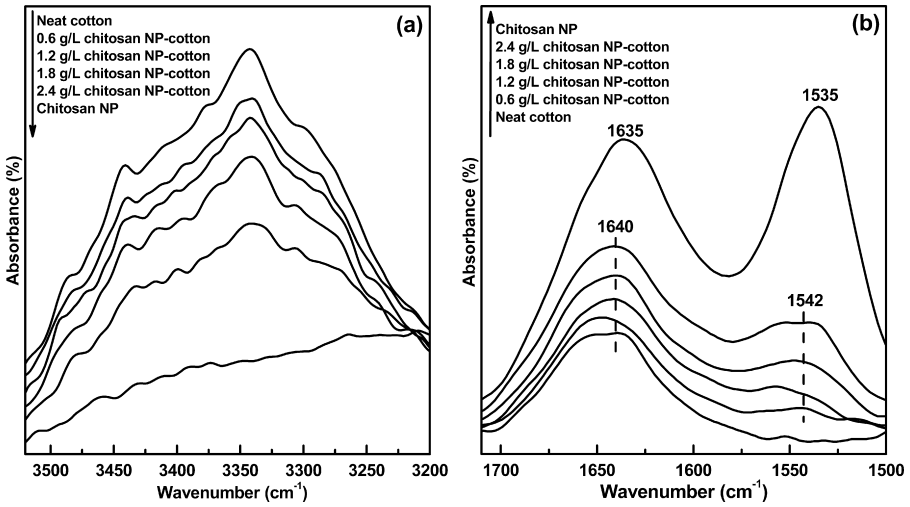

Fig. 1. FTIR spectra of chitosan NP, neat cotton and chitosan NP-cotton treated with different chitosan NP mass concentrations in the range of (a) 3520–3200 cm^{-1} and (b) 1710–1500 cm^{-1}.

the C=O stretching vibration of acetyl groups and the N—H bending vibration of amino groups (Papadimitriou et al., 2008), respectively. In the spectrum of chitosan NP-cotton, the N—H absorption band of amino groups was shifted to 1542 cm^{-1} after adsorption. Furthermore, the intensity of the band progressively enhanced with the increase in the content of chitosan NP. These results further indicated that the intermolecular hydrogen bonding interactions existing between cotton fibers and chitosan NP progressively augmented with the increasing chitosan NP mass concentration, and the amino groups of chitosan NP took part in the formation of these hydrogen bonds (Chen, Dong, & Cheung, 2005; De Mesquita et al., 2010).

3.2. XPS analysis

High resolution N1s XPS spectra of neat cotton and chitosan NP-cotton treated with different chitosan NP mass concentrations were shown in Fig. 2. An obvious N1s signal ranging from 403 to 397 eV was appeared in all chitosan NP-cotton samples after adsorption. The major peak occurring at 399.5 eV was attributed to the nitrogen atoms which were bonded to carbon atoms or the non-protonated amine groups (Matienzo & Winnacker, 2002). The minor peak occurring at 401.6 eV was belonged to the oxidized nitrogen atoms or the protonated amine groups (Dambies, Guimon, Yiacoumi, & Guibal, 2001; Matienzo & Winnacker, 2002). With the rising content of chitosan NP, the intensity of N1s signals enhanced accordingly, thus implying an increasing adsorption of chitosan NP onto cotton fibers.

The high resolution C1s XPS data were utilized to further consider the interactions between chitosan NP and cotton fibers. The C1s spectra were resolved into three peaks of different intensities as shown in Fig. 3. The peak C1 at 282.2 eV was assigned to C—C or C—H bonds. The peak C2 occurring at 284.0 eV was due to C—O or C—OH bonds. The last peak C3 at 285.3 eV was attributed to C=O or O—C—O bonds. This was consistent with previous studies on XPS analyses of the cotton fabric or cellulose (An, Wang, Li, & Huang, 2009; Freudenberg et al., 2005; Kontturi, Thüne, &

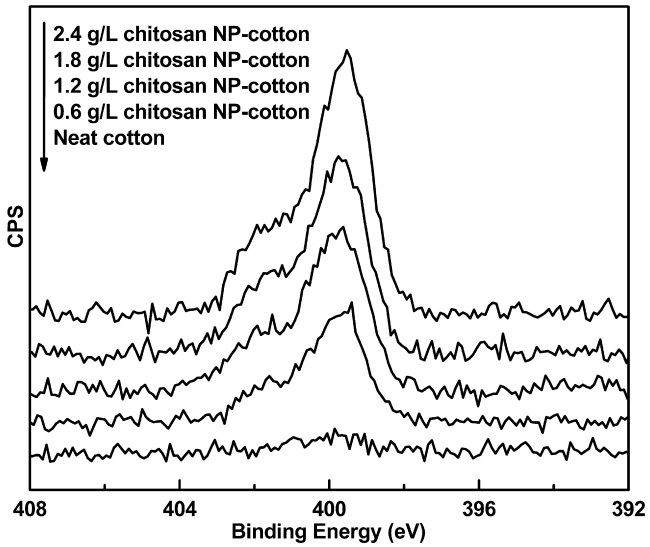

Fig. 2. High resolution XPS spectra of the N1s peak of neat cotton and chitosan NP-cotton treated with different chitosan NP mass concentrations.

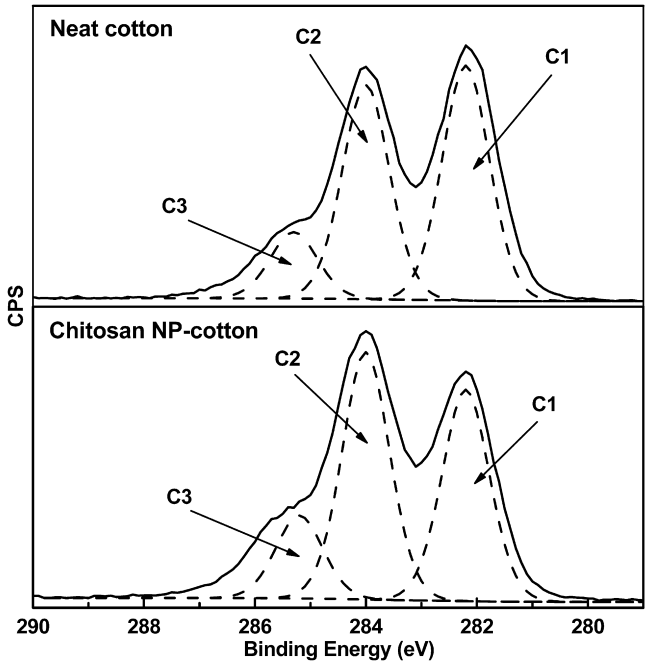

Fig. 3. High resolution XPS spectra of the C1s peak of neat cotton and chitosan NP-cotton treated with the chitosan NP mass concentration of 1.8 g/L.

Table 1
The relative peak areas and ratios obtained from the C1s XPS spectra of neat cotton and chitosan NP-cotton.

Sample	Relative peak areas (%)			Ratios (%)
	C1	C2	C3	C2/(C1 + C3)
Neat cotton	45.6	41.5	12.9	0.71
0.6 g/L chitosan NP-cotton	44.3	42.4	13.3	0.73
1.2 g/L chitosan NP-cotton	42.1	43.2	14.7	0.76
1.8 g/L chitosan NP-cotton	39.0	45.7	15.3	0.84
2.4 g/L chitosan NP-cotton	37.8	46.8	15.4	0.88

Niemantsverdriet, 2003). From the spectra in Fig. 3, the peak C2 and C3 increased with the respect to C1 after adsorption. The relative areas and ratios of C1, C2 and C3 peaks in the C1s spectra of various chitosan NP-cotton samples were presented in Table 1. As the chitosan NP mass concentration increased, the peak areas of C2 and C3 gradually augmented but the area of C1 peak decreased, consequently resulting in the increasing C2/(C1 + C3) ratio. According to the previous study, the peak C2 was related to the acidity of fibers, and the peaks of C1 and C3 were corresponded to their basicity (Shen, Mikkola, & Rosenholm, 1998). Therefore, the acidity of cotton fibers augmented due to chitosan NP adsorption. This finding further evidenced the hydrogen bonding interaction took place between chitosan NP, as the proton donors, and cotton fibers and enhanced with the increasing chitosan NP mass concentration, thereby resulting in the increase in the acidity of cotton fibers.

3.3. XRD analysis

In Fig. 4 the XRD patterns of chitosan NP, neat cotton and chitosan NP-cotton treated with different chitosan NP mass concentrations were shown. In the pattern of neat cotton, three significant diffraction peaks were appeared at a 2θ angle of 14.8°, 16.4° and 22.6° corresponding to (1 $\bar{1}$ 0), (1 1 0), and (2 0 0) crystallographic planes of cellulose I_β, respectively (Isogai, Usuda, Kato, Uryu, & Atalla, 1989). A weak and broad reflection from 15° to 30° was appeared in chitosan NP, which was agreement with the literature (Puttipipatkhachorn, Nunthanid, Yamamoto, & Peck, 2001). As the content of chitosan NP increased, the diffraction peaks of chitosan NP-cotton weakened and no additional reflections displayed, thus implying the decline of the fiber crystallinity. The calculated crystallinity index (*CrI*) and *d*-spacing of different cotton samples were presented in Table 2. A modest decrease in the value of *CrI* was observed with the increase in chitosan NP mass concentrations. This fact could be explained by a slight penetration of nanoparticles between the fiber chains leading to a less dense and less ordered structure (Ciolacu, Kovac, & Kokol, 2010), and the effects by increasing hydrogen bonds between chitosan NP and cotton fibers. However, the *d*-spacing values of all crystallographic planes hardly varied after adsorption, indicating the unit cell of cotton fiber was not changed after chitosan NP treatment. After adsorption, a more obvious decline of the diffraction peak belonging to the hydrophobic (2 0 0) crystallographic plane was observed comparing with the peaks of the hydrophilic (1 $\bar{1}$ 0) and (1 1 0) crystallographic plane. This finding confirmed that chitosan NP preferentially adsorbed onto the (2 0 0) crystallographic planes of cotton fibers due to the hydrophobic interactions between them (Ciolacu et al., 2010).

3.4. TG-DTG analysis

In Fig. 5 the TG and DTG curves of chitosan NP, neat cotton and chitosan NP-cotton treated with different chitosan NP mass concentrations were shown. From the TG curves in Fig. 5a, the minor

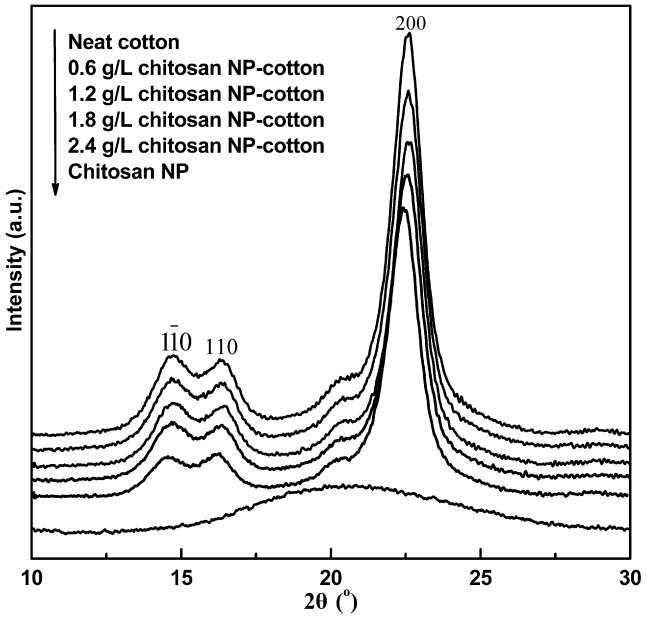

Fig. 4. XRD patterns of chitosan NP, neat cotton and chitosan NP-cotton treated with different chitosan NP mass concentrations.

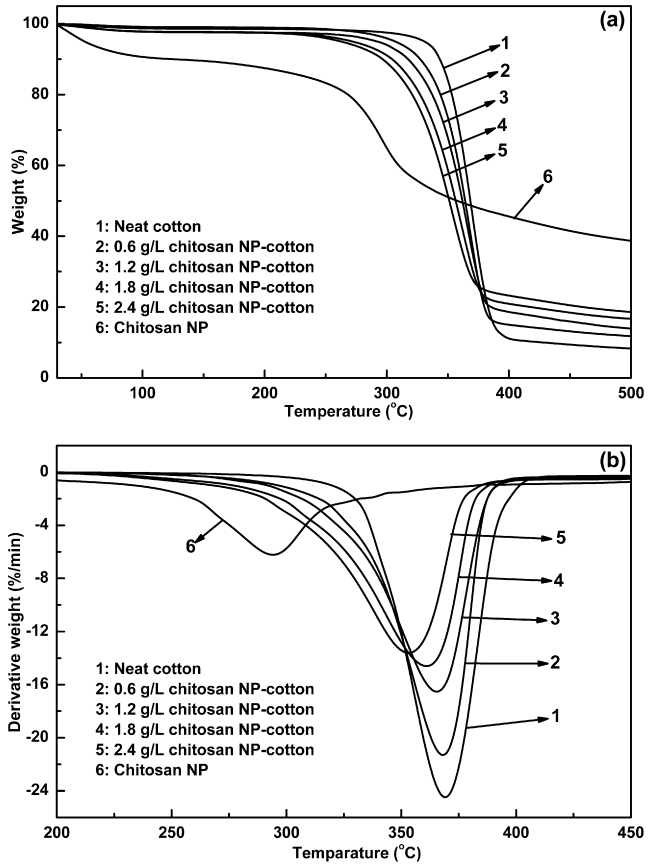

Fig. 5. TG curves (a) and DTG curves (b) of chitosan NP, neat cotton and chitosan NP-cotton treated with different chitosan NP mass concentrations.

Table 2
The crystallinity index (*CrI*) and *d*-spacing of neat cotton and chitosan NP-cotton.

Sample	*CrI* (%)	*d*-Spacing (nm)		
		$(1\ \bar{1}\ 0)$	(1 1 0)	(2 0 0)
Neat cotton	64.6	0.604	0.539	0.393
0.6 g/L chitosan NP-cotton	63.7	0.595	0.536	0.390
1.2 g/L chitosan NP-cotton	62.5	0.600	0.536	0.394
1.8 g/L chitosan NP-cotton	61.1	0.596	0.535	0.390
2.4 g/L chitosan NP-cotton	59.7	0.612	0.548	0.399

weight losses observed at 30–100 °C were related to the evaporation of the moisture from samples. The major weight losses of chitosan NP and cotton fibers observed at 200–400 °C were attributed to the decomposition of the chitosan and cellulose. After adsorption, the TG curves of chitosan NP-cotton shifted to low temperature and exhibited an decreasing weight loss with the increase in chitosan NP mass concentrations. The finding indicated that the content of chitosan NP adsorbed on cotton fiber surfaces progressively increased with the rising chitosan NP mass concentration. As can be seen from the DTG curves in Fig. 5b, a single peak of the maximum decomposition rate was observed at 294 and 370 °C in chitosan NP and neat cotton, respectively. In the DTG curves of chitosan NP-cotton, the peak temperature was reduced from 368 to 353 °C, accompanying with a declining peak intensity, when the chitosan NP mass concentration changed from 0.6 to 2.4 g/L. This result was related to the content changes of the nanoparticles adsorbed on cotton fibers according to the TG curves. Meanwhile, if there were no interactions between chitosan NP and cotton fibers, the derivative weight peaks should remain sharp and well defined. However, the reflection of chitosan NP at 294 °C disappeared in all curves of chitosan NP-cotton samples after adsorption. This fact provided an additional evidence for the formation of the intermolecular hydrogen bonds between chitosan NP and cotton fibers during the green adsorption.

3.5. SEM analysis

The morphologies of neat cotton and chitosan NP-cotton treated with different chitosan NP mass concentrations were shown in Fig. 6. It could be observed that the neat cotton showed a smoother

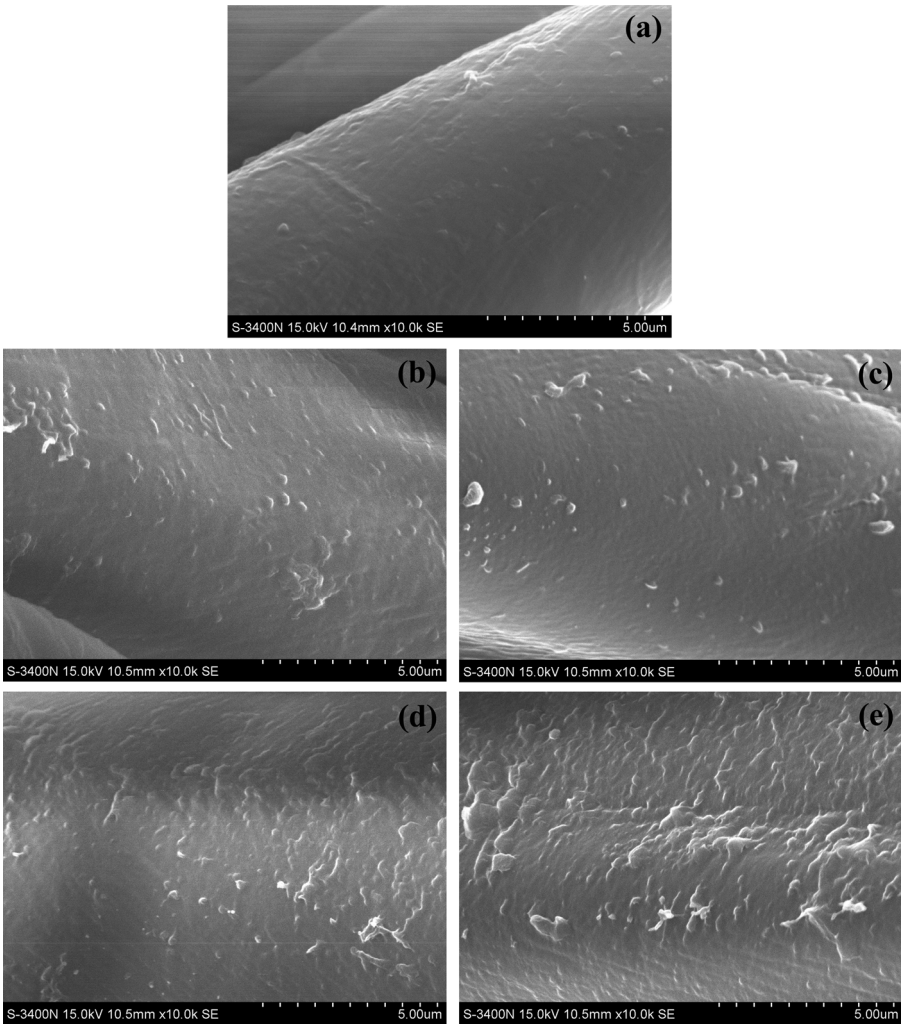

Fig. 6. SEM images of (a) neat cotton and chitosan NP-cotton treated with different chitosan NP mass concentrations: (b) 0.6 g/L, (c) 1.2 g/L, (d) 1.8 g/L, (e) 2.4 g/L.

surface than chitosan NP-cotton. After chitosan NP treatment, the nanoparticles of 200–300 nm appeared and spread over the cotton fiber surfaces, thus indicating chitosan NP could be coated on cotton fibers during the green adsorption. With the increase in chitosan NP mass concentrations, the amount of chitosan NP adsorbed on the cotton fibers progressively increased. Meanwhile, the spherical nanoparticels (Calvo et al., 1997; Hu et al., 2012) were incorporated onto the fiber surface and deformed their shapes to flat structure under a high chitosan NP mass concentration (above 1.8 g/L). These results showed certain interactions existed between chitosan NP and cotton fibers and enhanced with the increasing content of chitosan NP during adsorption, thus confirming the results obtained from the FTIR, XRD, XPS and TG-DTG analysis.

4. Conclusion

From the foregoing discussions, it appeared that certain interactions took place between chitosan NP and cotton fibers during a green adsorption. The FTIR and XPS results indicated the intermolecular hydrogen bonds were formed between the amino groups of chitosan NP and the hydroxyl groups of cotton fibers, and gradually enhanced with the rising chitosan NP mass concentration. From the XPS and XRD analysis, an increase in the acidity and a decrease in the crystallinity index of cotton fibers after chitosan NP adsorption were evidenced, proving the presence of the increasing interactions. The XRD measurements showed chitosan NP had different affinities for various crystallographic planes of cotton fibers, and a preference for adsorbing on the (2 0 0) crystallographic plane, demonstrating the hydrophobic interactions existed during adsorption. In addition, the TG-DTG results further confirmed the formation of hydrogen bonds between chitosan NP and cotton fibers. Based on these interactions, chitosan NP could be adsorbed onto cotton fibers surfaces effectively without any cross-linking agents, which was confirmed also by the SEM analysis.

Acknowledgments

The authors acknowledge for the financial supports from the Key Program and the General Program of National Natural Science Foundation of China (Nos. 21036009, 21076125, 21276157, and 21276006); the National Key Technology R & D Program of China (No. 2011BAD23B01); the Shanghai Committee of Science and Technology “Mountaineering Plan” International Cooperation Program (No. 11290707600); the Project of Shanghai Engineering Research Center for Flavors and Fragrances (No. 12DZ2251400) and the Funding Project for Academic Human Resources Development in Institutions of Higher Learning under the jurisdiction of the Beijing Municipality (No. PHR201107104).

References

An, Q., Wang, Q., Li, L., & Huang, L. (2009). Study of amino functional polysiloxane film on regenerated cellulose substrates by atomic force microscopy and X-ray photoelectron microscopy. *Textile Research Journal*, *79*, 89–93.

Bashar, M. M., & Khan, M. A. (2013). An overview on surface modification of cotton fiber for apparel use. *Journal of Polymers and the Environment*, *21*, 181–190.

Calvo, P., Remuñán-López, C., Vila-Jato, J. L., & Alonso, M. J. (1997). Novel hydrophilic chitosan–polyethylene oxide nanoparticles as protein carriers. *Journal of Applied Polymer Science*, *63*, 125–132.

Chen, C., Dong, L., & Cheung, M. K. (2005). Preparation and characterization of biodegradable poly(L-lactide)/chitosan blends. *European Polymer Journal*, *41*, 958–966.

Ciolacu, D., Kovac, J., & Kokol, V. (2010). The effect of the cellulose-binding domain from clostridium cellulovorans on the supramolecular structure of cellulose fibers. *Carbohydrate Research*, *345*, 621–630.

Dambies, L., Guimon, C., Yiacoumi, S., & Guibal, E. (2001). Characterization of metal ion interactions with chitosan by X-ray photoelectron spectroscopy. *Colloids and Surfaces A: Physicochemical and Engineering Aspects*, *177*, 203–214.

Da Róz, A. L., Leite, F. L., Pereiro, L. V., Nascente, P. A. P., Zucolotto, V., Oliveira, O. N., Jr., et al. (2010). Adsorption of chitosan on spin-coated cellulose films. *Carbohydrate Polymers*, *80*, 65–70.

De Mesquita, J. P., Donnici, C. L., & Pereira, F. V. (2010). Biobased nanocomposites from layer-by-layer assembly of cellulose nanowhiskers with chitosan. *Biomacromolecules*, *11*, 473–480.

Freudenberg, U., Zschoche, S., Simon, F., Janke, A., Schmidt, K., Behrens, S. H., et al. (2005). Covalent immobilization of cellulose layers onto maleic anhydride copolymer thin films. *Biomacromolecules*, *6*, 1628–1634.

Gan, Q., Wang, T., Cochrane, C., & McCarron, P. (2005). Modulation of surface charge, particle size and morphological properties of chitosan–TPP nanoparticles intended for gene delivery. *Colloids and Surfaces B: Biointerfaces*, *44*, 65–73.

Hejazi, R., & Amiji, M. (2003). Chitosan-based gastrointestinal delivery systems. *Journal of Controlled Release*, *89*, 151–165.

Hu, J., Xiao, Z., Ma, S., Zhou, R., Wang, M., & Li, Z. (2012). Properties of osmanthus fragrance-loaded chitosan–sodium tripolyphosphate nanoparticles delivered through cotton fabrics. *Journal of Applied Polymer Science*, *123*, 3748–3754.

Isogai, A., Usuda, M., Kato, T., Uryu, T., & Atalla, R. H. (1989). Solid-state CP/MAS carbon-13 NMR study of cellulose polymorphs. *Macromolecules*, *22*, 3168–3172.

Ivanova, N. A., & Philipchenko, A. B. (2012). Superhydrophobic chitosan-based coatings for textile processing. *Applied Surface Science*, *263*, 783–787.

Katas, H., & Alpar, H. O. (2006). Development and characterisation of chitosan nanoparticles for siRNA delivery. *Journal of Controlled Release*, *115*, 216–225.

Kontturi, E., Thüne, P. C., & Niemantsverdriet, J. W. (2003). Cellulose model surfaces simplified preparation by spin coating and characterization by X-ray photoelectron spectroscopy, infrared spectroscopy, and atomic force microscopy. *Langmuir*, *19*, 5735–5741.

Lehr, C. M., Bouwstra, J. A., Schacht, E. H., & Junginger, H. E. (1992). In vitro evaluation of mucoadhesive properties of chitosan and some other natural polymers. *International Journal of Pharmaceutics*, *78*, 43–48.

Li, Q., Zhou, J., & Zhang, L. (2009). Structure and properties of the nanocomposite films of chitosan reinforced with cellulose whiskers. *Journal of Polymer Science Part B: Polymer Physics*, *47*, 1069–1077.

Matienzo, L. J., & Winnacker, S. K. (2002). Dry processes for surface modification of a biopolymer: chitosan. *Macromolecular Materials and Engineering*, *287*, 871–880.

Muzzarelli, R. A. A. (2012). Nanochitins and nanochitosans, paving the way to eco-friendly and energy-saving exploitation of marine resources. In K. Matyjaszewski, & M. Möller (Eds.), *Polymer science: A comprehensive reference* (Vol. 10) (pp. 153–164). Amsterdam: Elsevier BV.

Muzzarelli, R. A. A., Boudrant, J., Meyer, D., Manno, N., DeMarchis, M., & Paoletti, M. G. (2012). Current views on fungal chitin/chitosan, human chitinases, food preservation, glucans, pectins and inulin: A tribute to Henri Braconnot, precursor of the carbohydrate polymers science, on the chitin bicentennial. *Carbohydrate Polymers*, *87*, 995–1012.

Papadimitriou, S., Bikiaris, D., Avgoustakis, K., Karavas, E., & Georgarakis, M. (2008). Chitosan nanoparticles loaded with dorzolamide and pramipexole. *Carbohydrate Polymers*, *73*, 44–54.

Phisalaphong, M., & Jatupaiboon, N. (2008). Biosynthesis and characterization of bacteria cellulose–chitosan film. *Carbohydrate Polymers*, *74*, 482–488.

Puttipipatkhachorn, S., Nunthanid, J., Yamamoto, K., & Peck, G. E. (2001). Drug physical state and drug–polymer interaction on drug release from chitosan matrix films. *Journal of Controlled Release*, *75*, 143–153.

Rajendran, R., Radhai, R., Kotresh, T. M., & Csiszar, E. (2013). Development of antimicrobial cotton fabrics using herb loaded nanoparticles. *Carbohydrate Polymers*, *91*, 613–617.

Rosca, C., Popa, M. I., Lisa, G., & Chitanu, G. C. (2005). Interaction of chitosan with natural or synthetic anionic polyelectrolytes. 1. The chitosan–carboxymethylcellulose complex. *Carbohydrate Polymers*, *62*, 35–41.

Rous, M. A., Ingolic, E., & Schuster, K. C. (2006). Visualisation of the fibrillar and pore morphology of cellulosic fibres applying transmission electron microscopy. *Cellulose*, *13*, 411–419.

Saboktakin, M. R., Tabatabaee, R. M., Maharramov, A., & Ramazanov, M. A. (2010). Design and characterization of chitosan nanoparticles as delivery systems for paclitaxel. *Carbohydrate Polymers*, *82*, 466–471.

Shen, Q., Mikkola, P., & Rosenholm, J. B. (1998). Quantitative characterization of the subsurface acid–base properties of wood by XPS and Fowkes theory. *Colloids and Surfaces A: Physicochemical and Engineering Aspects*, *145*, 235–241.

Ul-Islam, M., Shah, N., Ha, J. H., & Park, J. K. (2011). Effect of chitosan penetration on physico-chemical and mechanical properties of bacterial cellulose. *Korean Journal of Chemical Engineering*, *28*, 1736–1743.

Vila, A., Sánchez, A., Tobío, M., Calvo, P., & Alonso, M. J. (2002). Design of biodegradable particles for protein delivery. *Journal of Controlled Release*, *78*, 15–24.

Watanabe, A., Morita, S., Kokot, S., Matsubara, M., Fukai, K., & Ozaki, Y. (2006). Drying process of microcrystalline cellulose studied by attenuated total reflection IR spectroscopy with two-dimensional correlation spectroscopy and principal component analysis. *Journal of Molecular Structure*, *799*, 102–110.

Wu, Y. B., Yu, S. H., Mi, F. L., Wu, C. W., Shyu, S. S., Peng, C. K., et al. (2004). Preparation and characterization on mechanical and antibacterial properties of chitosan/cellulose blends. *Carbohydrate Polymers*, *57*, 435–440.

Ye, W., Xin, J. H., Li, P., Lee, K. D., & Kwong, T. (2006). Durable antibacterial finish on cotton fabric by using chitosan-based polymeric core–shell particles. *Journal of Applied Polymer Science*, *102*, 1787–1793.

Zhang, H., Oh, M., Allen, C., & Kumacheva, E. (2004). Monodisperse chitosan nanoparticles for mucosal drug delivery. *Biomacromolecules*, *5*, 2461–2468.